Fatigue induces behavioural improvements in the unfatigued hand via altered functional connectivity and neurochemicals in cortical motor areas

Justin W. Andrushko[1,2], Jacob M. Levenstein[2,3], Catharina Zich[2,4], Evan C. Edmond[2], Jon Campbell[2], William T. Clarke[2], Uzay Emir[5], Jonathan P. Farthing[1*], Charlotte J. Stagg[2*]

1. College of Kinesiology, University of Saskatchewan, Canada
2. Wellcome Centre for Integrative Neuroimaging, FMRIB, Nuffield Department of Clinical Neurosciences, University of Oxford, United Kingdom
3. Section on Functional Imaging Methods, National Institutes of Mental Health, National Institutes of Health, Bethesda, Maryland, United States
4. Department of Clinical and Movement Neurosciences, University College London, United Kingdom
5. School of Health Sciences, College of Health and Human Sciences, Purdue University, United States

* Co-senior authors

Correspondence

Dr. Justin W. Andrushko, PhD

Justin.andrushko@usask.ca

ORCID: https://orcid.org/0000-0003-2258-1689

Keywords

resting-state functional connectivity, handgrip, serial reaction time, cross-education, motor learning

Key points summary

- Right handgrip contractions at 50% MVC improve left hand response times.
- Repeated handgrip contractions at 50% MVC alter interhemispheric functional connectivity.
- Unilateral exercise may be an effective method for enhancing contralateral limb motor performance in rehabilitation settings.

Data sharing

All data will be available from the authors upon reasonable request.

Abstract

In humans, motor learning is underpinned by changes in functional connectivity (FC) across the sensorimotor network. Unilateral exercise-induced fatigue increases FC in the ipsilateral primary motor cortex (M1) and supplementary motor area (SMA); areas involved in motor planning and execution of the contralateral hand. Unilateral fatiguing exercise is therefore a promising potential approach to augment motor performance in the non-fatigued, contralateral, hand. In a within-participant, controlled, randomized, cross-over design, 15 right-handed adults had two magnetic resonance imaging (MRI) sessions, where functional MRI and MR Spectroscopic Imaging were acquired before and after repeated right-hand contractions at either 5% or 50% maximum voluntary contraction (MVC). Before and after scanning, response times (RTs) were determined in both hands, and after scanning, participants performed a serial reaction time task (SRTT) with their left, unfatigued, hand. Nine minutes of 50% MVC contractions resulted in fatigue. This unimanual fatigue improved motor performance, as indexed by decreased RTs, in the contralateral hand. Although fatigue had no significant effects on sequence learning, fatigue led to a significant increase in the transfer of the learned skill to the untrained hand. These behavioural effects were supported by significant neural changes: an increase in SMA-SMA functional connectivity, and increased connectivity between right M1 and right Orbitofrontal Cortex. At a neurochemical level, the degree of fatigue-induced decrease in GABA in left M1, left and right SMA correlated with subsequent behavioural improvements in the left-hand. These results support unilateral fatiguing exercise as a potential therapeutic intervention in a range of neurological and orthopedic conditions.

Introduction

The acquisition of motor skill is essential in our daily lives. Able-bodied individuals may take for granted the abilities to grasp and manipulate objects, or even to safely complete essential activities of daily living. However, many people lose their ability to perform these tasks through a variety of injuries. Restoring function in these individuals is of clear clinical importance, but *how* we can optimally improve behaviour is an open scientific question: both in terms of restoring motor function in orthopedic or neurologically impaired individuals such as stroke survivors, and in healthy populations, such as athletes, looking to maximize motor performance.

One approach showing particular promise to enhance motor skill acquisition is cross-education (CE). CE describes the phenomenon by which unilateral exercise enhances muscle activity, force generation, or skill in the contralateral, homologous muscle (Manca *et al.*, 2021). CE is effective in preserving muscle strength and size in an immobilized limb (Farthing *et al.*, 2009, 2011; Magnus *et al.*, 2010; Pearce *et al.*, 2013; Andrushko *et al.*, 2018; Valdes *et al.*, 2021), and strength and range of motion of a fractured arm (Magnus *et al.*, 2013) when the unaffected limb is trained. Studies have also found CE to be effective for motor recovery in chronic stroke survivors (Dragert & Zehr, 2013; Urbin *et al.*, 2015; Sun *et al.*, 2018; Dehno *et al.*, 2021).

Current evidence suggests cortical mechanisms likely drive CE effects (Ruddy & Carson, 2013; Manca *et al.*, 2018), although it is not yet clear *how* these inter-hemispheric behavioural transfer effects occur. At a systems level studies suggest fatiguing exercise increases functional connectivity in the sensorimotor network, particularly in the ipsilateral (unfatigued) M1 (iM1), ipsilateral SMA, and contralateral SMA (Jiang *et al.*, 2012), and enhances muscle activity in the contralateral unfatigued homologous muscle (Carr *et al.*, 2021). Similarly, high force exercise, which is known to produce large CE effects (Urbin *et al.*, 2015; Pelet & Orsatti, 2021), also increases functional connectivity in the ipsilateral hemisphere (Andrushko *et al.*, 2021).

At a neurochemical level, unilateral fatiguing exercise decreases iM1 $GABA_A$ activity, as quantified by the Transcranial Magnetic Stimulation protocol Short Intracortical Inhibition (SICI; (Maruyama *et al.*, 2006; Ni *et al.*, 2007; Takahashi *et al.*, 2009)). GABAergic inhibition decreases during motor learning (Floyer-Lea *et al.*, 2006; Kolasinski *et al.*, 2019), and the magnitude of this GABA decrease correlates with the extent of subsequent motor learning (Stagg *et al.*, 2011*a*). Indeed, decreasing M1 GABA using non-invasive brain stimulation techniques increases motor skill acquisition, both in healthy adults (Reis *et al.*, 2009; Stagg *et al.*, 2011*b*) and in functional recovery after stroke (Kim *et al.*, 2010; Allman *et al.*, 2016).

Considering motor network connectivity is at least in part controlled by M1 inhibition (Stagg *et al.*, 2014; Bachtiar *et al.*, 2015), here we acquire two independent measures to test the hypothesis that fatigue increases motor performance in the unfatigued hand by increasing interhemispheric homologous connectivity of M1 and SMA, via an altered inhibitory/excitatory state within these cortical motor regions by increasing glutamate and/or decreasing GABA (figure 1A).

Methods

This study conforms to the Declaration of Helsinki and was approved by the Oxford Central University Research Ethics Committee (MSD-IDREC-C1-2014-100 and MSD-IDREC-C1-2014-090). Using an effect of $\eta^2 = 0.250$ based on a previous work (Bachtiar *et al.*, 2018), we computed an estimated total sample size of 12 (G*Power 3.1.9.2; $1-\beta = 0.95$, $\alpha = 0.05$). To allow for dropout and data loss, we therefore recruited fifteen right-handed participants aged between 18-35 years (28.92 ± 3.30 years; 7 Female). Exclusion criteria were: playing a musical instrument to Associated Board of the Royal Schools of Music Grade 5 or higher, any contraindication to MRI, any history of neurological or psychiatric disorders.

Experimental Outline

Participants had two experimental sessions where they performed a right handgrip force-matching task at either 5% or 50% of their maximum voluntary contraction (MVC). During each experimental session, response times (RTs) of each hand were assessed before and after the MRI. Resting-state functional MRI (fMRI) and magnetic resonance spectroscopic imaging (MRSI) scans were acquired before and after a nine minute right handgrip force-matching task at either 5% or 50% MVC. Finally, outside the scanner participants performed a serial reaction time task (SRTT) with their left hand, which consisted of three separate segments, interspersed with two minutes of the same right handgrip force-matching task as in the scanner. This study had a within-participant repeated measures design, with the order of conditions stratified-randomized for sex across the group (figure 1B).

Handgrip force-matching task

The handgrip force-matching task was performed using an MRI-compatible hand dynamometer (Biopac Systems Inc. Aero Camino Goleta, CA) and implemented using in-house code (Psychtoolbox-3 (Kleiner *et al.*, 2007; The Mathworks Inc, 2018)). Participants performed a visually cued 0.5 Hz (1 second contraction, 1 second rest) repeated force-matching task at either 5% or 50% of their MVC, depending on the session. The target force was displayed halfway up the vertical axis, and participants were instructed to squeeze the dynamometer to guide a cursor up the screen until it reached the target. During scanning, participants performed 273 handgrip contractions over the nine-minute task. During the post-MRI motor learning component of the study, participants performed 4 blocks of 62 contractions each, which were interleaved with the SRTT task.

Handgrip force-matching task analysis

The area under the curve (AUC) of the contraction force was calculated over a two second window for every contraction separately. For each participant (and session) a regression line was then fitted to the AUC measures across all contractions for each participant and session

separately. The β of the regression from each session was used to quantify motor performance, whereby a $\beta < 0$ indicates a decrement in motor performance over time, consistent with fatigue.

Serial reaction time task

Participants performed a visually-cued serial reaction time task before and after MRI scanning, implemented in PsychoPy3 (Peirce et al., 2019). Participants responded via a button box (4-Button Inline, HHSC-1x4-L; Current Designs Inc. Philadelphia, PA USA) with their right or left hand depending on the block. The task was divided into blocks of 64 self-paced visual cues, which participants were asked to respond to by pressing the corresponding button on the button box as quickly and accurately as possible.

In random blocks, cues were presented in a pseudo-random order. In sequence blocks, the cues consisted of a 16-button sequence repeated four times. Participants were not told about the presence of a sequence. Different sequences were used for each session and the order was counter-balanced across the participants.

With each hand separately, participants performed two random blocks at the Pre-MRI Baseline and Post-MRI timepoints. They then performed three learning segments with their left hand each following the two-minute submaximal handgrip force-matching task with the right hand. Each learning segment started with a random block, followed by four sequence blocks. The post-learning timepoint consisted of three blocks (Random, Sequence, Random), performed separately with their right and left hands. Finally, following a 15-minute break, retention of the trained motor sequence was assessed identically to the post-learning timepoint (figure 1B).

SRTT analysis

Incorrect button-press responses, and RTs < 50 ms or > 700 ms were removed. The median response time of the remaining button presses was then calculated for each block separately. To investigate changes in RT due to fatigue, the percent change in RTs for each hand was calcu-

lated using the mean of the medians from the two baseline blocks as the Pre-MRI value, and similarly, the mean of the medians from the two Post-MRI blocks was used as the Post-MRI value.

To assess learning, we performed a RM-ANOVA with one factor of condition (5% MVC, 50% MVC) and one factor of time (15 blocks). At the post-learning and retention timepoints, we compared the median RT in the sequence block to the mean of the median RTs of the two random blocks.

To investigate any significant change in RT between Baseline and Post-MRI, we performed a RM-ANOVA using the percent change in RT data with one factor of condition and another of hand.

Magnetic Resonance Imaging

MRI sessions were acquired using a Siemens 3-tesla Prisma whole-body MRI scanner with a 32-channel head array receive coil (Siemens, Erlangen, Germany). T1-weighted MPRAGE scans (voxel size 1 mm^3, TR = 1900 ms, TI = 912 ms TE = 3.96 ms, FOV = 232 × 256 × 192 mm^3, flip angle = 8°, TA = 7:21) were acquired for registration purposes and to guide placement of the MRSI slab, prioritising left M1. Pre- and Post-task resting-state semi-LASER localised density-weighted concentric-ring trajectory MRSI (voxel size 5 mm × 5 mm × 15 mm, semi-LASER VoI 85 mm x 35 mm x 15 mm, TR = 1400 ms, TE = 32 ms, FOV = 240 mm × 240 mm × 15 mm, TA = 4:30) (Steel *et al.*, 2018), and fMRI (490 volumes, voxel size 2.4 mm^3 with zero gap, TR = 735 ms, TE = 39 ms, FOV = 210 × 210 × 154 mm, flip angle = 52°, TA = 6:10) (Miller *et al.*, 2016) data were acquired. Participants were asked to fixate on a grey cross presented on a black screen and to blink normally. To quantify any potential change in head position after task performance a single localiser (voxel size 1.4 mm, TR = 3.15 ms, TE = 1.37 ms, FOV = 350 mm × 350 mm × 263 mm, 128 slices, flip angle = 8°, TA = 0:22) was collected prior to Post-task MRSI. Finally, B_0 field maps (voxel size 2 mm^3, TR = 482 ms, TE1 = 4.92 ms, TE2 = 7.38 ms, FOV = 216 mm × 216 mm ×

146 mm, 49 slices, flip angle = 46°, TA = 1:45) were acquired to correct for field distortion in the resting-state fMRI data.

MRI analysis

fMRI preprocessing

Functional MRI analyses were performed using tools from the FMRIB Software Library (FSL v6.0.3; (Jenkinson *et al.*, 2012)). Standard preprocessing steps were performed, including removal of non-brain tissue (BET; (Smith, 2002)), removal of the initial two volumes, motion correction (MCFLIRT; (Jenkinson *et al.*, 2002)), high-pass temporal filtering at 0.01Hz, and distortion correction with the implementation of field-maps.

Following single-participant MELODIC pre-processing (v3.15), FMRIB's Independent Component Analysis (ICA)-based Xnoiseifier (ICA-FIX) was used to automatically denoise the data (Griffanti *et al.*, 2014; Salimi-Khorshidi *et al.*, 2014). The UK Biobank training-weights file (UKBiobank.RData) was used with a threshold value of 20, and 0.01Hz high-pass filtered motion confound cleanup. Following the automated denoising, all components were manually inspected before the cleaned data were smoothed with a 5 mm full-width half maximum (FWHM) kernel.

Individual resting state fMRI scans were first registered to the respective T1 structural scan using boundary-based registration as implemented in FMRIB's Linear Image Registration Tool (FLIRT; (Jenkinson & Smith, 2001; Jenkinson *et al.*, 2002)), and then to a standard space template (MNI152 2 mm) using non-linear registration (FNIRT; (Andersson *et al.*, 2007*a*, 2007*b*)).

fMRI analysis

We assessed resting state functional connectivity using two different approaches: (1) a seed-based functional connectivity approach to test the hypothesis that unimanual handgrip

contractions lead to changes in connectivity of the ipsilateral right M1 (rM1); and (2) a region of interest (ROI)-based functional connectivity analysis to specifically address our *a priori* hypothesis that unimanual fatigue would increase M1-M1 and SMA-SMA connectivity.

(1) Seed-based, whole-brain functional connectivity

The hand area of the unfatigued, rM1 was defined from previous functional MRI data of hand movements (Weinrich *et al.*, 2017), and the mean timeseries was extracted from this region for each participant and each session independently. This was then entered as a regressor into a lower-level FEAT analysis (Woolrich *et al.*, 2001), and task-related changes in functional connectivity of rM1 were investigated via a higher level mixed-effects analysis using a cluster forming threshold of $z = 3.1$ and $p = 0.05$ (Woolrich *et al.*, 2004).

(2) ROI-ROI-based functional connectivity

Next, we wanted to specifically assess changes in M1-M1 and SMA-SMA functional connectivity. The hand area of the M1s was functionally defined as above, and SMA was defined from tractography-based parcellation (Johansen-Berg *et al.*, 2004). The mean timeseries from within each region was extracted for each participant and session separately. We calculated the Pearson's r values between the homologous pairs using custom in-house MATLAB scripts, which were then converted to z-scores using a Fishers *r* to z transformation. The z-scores for the correlation between the homologous pairs were then used in a 2 × 2 × 2 (condition (5%, 50% MVC) × ROI (M1, SMA) × time (pre-task, post-task)) RM-ANOVA.

MRSI

MRSI data was reconstructed and pre-processed according to Steel et al. (2018), using in-house scripts. Reconstruction and pre-processing included: i. metabolite cycling reconstruction (Emir *et al.*, 2017), ii. coil-combination (Walsh *et al.*, 2000), iii. frequency and iv. phase shift correction, v. HLSVD for residual water removal (Cabanes *et al.*, 2001), and vi. eddy current correction using the unsuppressed water signal (Klose, 1990). Concentration of neurochemicals was quantified as in Steel et al. (2018) using LCModel (Provencher, 2001, 2016). A chemical shift of 0.5 to 4.2 ppm was evaluated with a basis set containing 20 metabolites and default LCModel macromolecules with disabled soft constraints on metabolites (NRATIO set to

0), and a baseline stiffness setting (DKMTM) of 0.25 (see Figure 5A for example of raw spectra and model fits). Each voxel spectrum was independently fit with spectral quality and assessment of model fitting performed using in-house scrips. For the metabolite maps of glutamate + glutamine (Glx) and GABA, MRSI voxels with CRLB values > 50 or SNR < 40 were excluded from further analysis. All metabolite measurements are expressed as a ratio over total Creatine (tCr).

Metabolite maps were next upsampled to $1mm^3$ resolution using nearest neighbour interpolation to preserve the original sampling grid. Metabolite maps were then aligned to their native T1 coordinate space. To correct for potential shift in head position, structural scans acquired prior to each MRSI sequence were aligned using McFLIRT (Jenkinson et al., 2002). The metabolite maps were then transformed using the McFLIRT generated registration matrix. Only shared MRSI voxels from within an intersection mask of QA-passed and head position-aligned MRSI voxels across each timepoint were included in subsequent analyses. For the ROI analysis, the four binary ROI masks [left M1 (lM1), right (rM1), left SMA (lSMA) and right SMA (rSMA)] were non-linearly aligned to native T1 space by inverse warping (3dNwarpApply) the native to standard space alignment, generated with @SSwarper (Cox, 1996; Saad et al., 2009; Cox & Glen, 2013). The native space ROIs were thresholded at 0.5 to mitigate partial volume effects. Within the intersection mask, mean concentration of Glx/tCr and GABA/tCr were then extracted for each of the four ROIs.

Statistical Analyses

Statistical analyses were run using Jamovi v1.6.9 (The Jamovi Project, 2020). Hedges' g effect sizes are reported for t-tests and partial eta squared (η_p^2) effect sizes are reported for ANOVA results. Greenhouse-Geisser corrections were applied as necessary where violations of sphericity were present.

Results

Performance of the 50% MVC handgrip force-matching task induced fatigue

We first wanted to determine if the 50% MVC handgrip force-matching task induced fatigue. We reasoned that the total grip force would be reduced over time during our 50% MVC fatiguing condition, but not during non-fatiguing movement in our 5% MVC control condition. We therefore quantified the AUC of the force profile for each condition separately and calculated a line of best fit for each participant for each session. In line with our hypothesis, 50% MVC showed a significant decrement in performance over time compared with 5% MVC (50% MVC: $\beta = -0.912 \pm 1.070$; 5% MVC: $\beta = -0.022 \pm 0.107$; slope of 50% MVC compared with zero: $t(14) = -3.302$, $p = 0.005$, $g = -0.824$; paired t-test $t(14) = 3.211$, $p = 0.006$, $g = 0.801$; figure 2A).

Right hand fatigue decreased RTs in the left, unfatigued hand

We next investigated whether performance of a 50% MVC fatiguing force-matching task with the right-hand would induce a behavioural improvement of the unfatigued, left-hand. After running a condition × hand RM-ANOVA with the RT percent change data, we observed a significant condition × hand interaction ($F(1,14) = 4.84$, $p = 0.045$, $\eta_p^2 = 0.257$), but no significant main effects. Next, to further understand the interaction we split the data by hand and ran paired sample t-tests between conditions for each hand. This revealed a significant difference between conditions for the left-hand ($t(14) = 2.30$, $p = 0.037$, $g = 0.574$), indicating the improvement in RTs for the 50% MVC condition ($\Delta = -5.85 \pm 7.05\%$) was different than the 5% MVC condition ($\Delta = 0.08 \pm 5.99\%$). Further, a one-sample t-test was used to determine the RT improvement in the left-hand for the 50% MVC condition was significantly different from zero ($t(14) = -3.21$, $p = 0.006$, $g = -0.801$). There were no significant differences for the right-hand between

the 50% MVC (Δ = -2.02 ± 4.35%) and 5% MVC (Δ = -0.73 ± 3.46%) conditions ($t(14)$= 0.788, p = 0.441, g = 0.196; figure 2B).

Fatigue increased transfer of learned sequence to the untrained hand

Next, we went on to address the hypothesis that right-hand fatigue would lead to CE, i.e., an increased rate of skill acquisition in the right, untrained hand after left-hand SRTT motor training.

As expected, participants were able to learn the SRTT with their left-hand, as shown by a decrease in RTs over time [RM-ANOVA with one factor of condition (5% MVC, 50% MVC) and one factor of block (1-15); significant main effect of block ($F(1.9,26.5) = 12.035$, $p < 0.001$, $\eta_p^2 = 0.462$); figure 3A]. However, there were no differences in learning between the two conditions [no significant main effect of condition ($F(1,14) = 0.595$, $p = 0.453$, $\eta_p^2 = 0.041$), no condition × block interaction ($F(4.2,59.1) = 0.836$, $p = 0.513$, $\eta_p^2 = 0.056$)]. At post-learning and retention separate condition × block type (random, sequence) RM-ANOVA tests were run for the left-hand. These analyses revelated significant main effects of block type at post-learning ($F(1,14) = 14.556$, $p = 0.002$, $\eta_p^2 = 0.510$) and retention ($F(1,14) = 12.739$, $p = 0.003$, $\eta_p^2 = 0.476$). However, the condition × block type interactions at post-learning ($F(1,14) = 0.815$, $p = 0.382$, $\eta_p^2 = 0.055$) and retention ($F(1,14) = 0.909$, $p = 0.357$, $\eta_p^2 = 0.061$), in addition to the main effect of condition at Post-Learning ($F(1,14) = 2.892$, $p = 0.111$, $\eta_p^2 = 0.171$) and Retention ($F(1,14) = 0.013$, $p = 0.909$, $\eta_p^2 = 0.001$) all were not significant. These data suggest that left-hand sequence learning occurred for both conditions, but no differences were observed between conditions (figure 3B).

Next, we asked whether the right-hand fatigue affected the ability to transfer the learned sequence from the trained left-hand to the untrained right-hand. We performed additional condition × block type RM-ANOVA tests at post-learning and retention for the untrained right-hand. As would be expected, participants were faster when performing the learned sequence than the random sequence [significant main effect of block type, ($F(1,14) = 8.155$, $p = 0.013$, η_p^2

= 0.368)]. However, there was a significant difference between the 50% and 5% MVC conditions in the degree of sequence transfer [significant condition × block type interaction ($F(1,14) = 6.325$, $p = 0.025$, $\eta_p^2 = 0.311$)], which was driven by faster response times in sequence, but not random, blocks in the 50% condition (50% MVC: sequence vs random blocks: $t(14) = 2.881$, $p = 0.012$, g = 0.719). However, by the retention timepoint there was no difference between the conditions (significant main effect of block type ($F(1,14) = 8.419$, $p = 0.012$, $\eta_p^2 = 0.376$), no significant main effect of condition ($F(1,14) = 0.377$, $p = 0.549$, $\eta_p^2 = 0.026$) and no significant condition × block type interaction ($F(1,14) = 0.797$, $p = 0.387$, $\eta_p^2 = 0.054$; figure 3B).

Fatigue increased functional connectivity between the ipsilateral rM1 and right orbitofrontal cortex

To investigate the neural changes associated with our observed fatigue-induced behavioural improvements in the unfatigued hand, we performed a voxel-wise seed-based analysis from the hand area of ipsilateral, rM1. There was a significant increase in functional connectivity with the ipsilateral, right orbitofrontal cortex (rOFC) in the 50% MVC condition (table 1; figure 4A).

SMA-SMA connectivity increased after fatiguing contractions

To address our *a priori* hypothesis that the 50% MVC condition would alter functional connectivity between M1 and SMA, we performed an ROI-ROI connectivity analysis between left and right M1 and SMA. A RM-ANOVA with one factor of condition (5% MVC, 50% MVC), one factor of ROI (M1, SMA), and one factor of time (Pre-Task, Post-Task) revealed a significant three-way (condition × ROI × time) interaction [($F(1,14) = 10.154$, $p = 0.007$, $\eta_p^2 = 0.420$; a significant main effect of ROI ($F(1,14) = 118.113$, $p < 0.001$, $\eta_p^2 = 0.894$), but no significant main effect of condition ($F(1,14) = 0.508$, $p = 0.488$, $\eta_p^2 = 0.8035$), or time ($F(1,14) = 0.797$, $p = 0.387$, $\eta_p^2 = 0.054$)].

To understand this three-way interaction, we then ran separate RM-ANOVA tests for the 50% and 5% MVC conditions, which revealed a significant ROI × time interaction for the 50% MVC condition ($F(1,14) = 11.970$, $p = 0.004$, $\eta_p^2 = 0.461$) but not for the 5% MVC condition ($F(1,14) < 0.001$, $p = 0.997$, $\eta_p^2 < 0.001$). Follow-up tests revealed that this interaction was driven by a significant change in SMA-SMA connectivity in the 50% MVC condition ($t(14) = -2.203$, $p = 0.045$, g = -0.550), figure 4B).

Given the 50% MVC force-matching task led to both fatigue and an increase in SMA-SMA connectivity, we next wanted to investigate whether these two effects were related. We demonstrated a negative correlation between the degree of fatigue in the 50% MVC condition and change in SMA-SMA connectivity, such that greater fatigue, indexed by greater decrease in the force output, correlated with an increase in SMA-SMA connectivity ($r^2_{adjusted} = 0.208$, $p = 0.050$, $\beta = -0.1572$; figure 4C). This correlation was both anatomically and behaviourally specific, such that this relationship was not observed for M1-M1 connectivity (50% MVC: M1-M1 connectivity and fatigue $r^2_{adjusted} = -0.077$, $p = 0.945$, $\beta = -0.076$) or in SMA-SMA connectivity in the 5% MVC condition (5% MVC: SMA-SMA connectivity and fatigue: $r^2_{adjusted} = -0.024$, $p = 0.427$, $\beta = -0.863$). Fishers r-to-z analysis determined that the correlations between M1-M1 (z = -0.45, $p = 0.65$) connectivity and SMA-SMA (z = 0.77, $p = 0.44$) connectivity with fatigue did not differ between conditions.

Decrease in SMA and M1 GABA correlated with decrease in left-hand RTs after fatigue

Finally, given our *a priori* hypothesis that the behavioural effects of fatigue are driving by changes in inhibition, we investigated changes in GABA within each ROI. We ran RM-ANOVA tests for M1 and SMA separately, with one factor of condition (50% MVC, 5% MVC), one factor of hemisphere (left, right) and one factor of time (pre, post). There were no significant main effects or interactions with condition. However, in line with our *a priori* hypothesis that GABA would decrease and Glx would increase on a participant-by-participant basis for the 50% MVC

condition only, there were significant positive relationships between a decrease in lM1 GABA (one-tailed: $r^2_{adjusted}$ = 0.196, p = 0.028, β = 4.79), lSMA GABA (one-tailed: $r^2_{adjusted}$ = 0.143, p = 0.045, β = 3.68), rSMA GABA (one-tailed: $r^2_{adjusted}$ = 0.172, p = 0.035, β =6.11) and the decrease in RTs for the unfatigued left-hand. A significant negative relationship was also observed for the increase in rM1 Glx with the decrease in RTs for the unfatigued left-hand (one-tailed: $r^2_{adjusted}$ = 0.167, p = 0.036, β = -2.69). These findings suggest that bilateral M1 and SMA alterations in inhibition and excitation predict the degree of RT improvement in the unfatigued hand (figure 5).

Discussion

The objective of this study was to determine the neural correlates of unimanual fatigue and the impact of fatigue on CE. Specifically, we hypothesised that fatigue would induce increased sensorimotor functional connectivity (Jiang *et al.*, 2012) and disinhibition of ipsilateral motor areas (Maruyama *et al.*, 2006, 2012; Takahashi *et al.*, 2009), neural effects that lead to enhanced performance of the contralateral, unfatigued, hand.

We showed that right handgrip contractions at 50% MVC, but not 5% MVC, resulted in fatigue. In line with the expected CE effects, this unilateral fatigue had behavioural effects: we observed decreased RTs in the left, unfatigued hand. These behavioural changes were accompanied by neural changes. We observed increased SMA-SMA connectivity, which correlated with the degree of fatigue on a participant-by-participant basis. Additionally, increased rM1-rOFC connectivity was observed on a voxel-wise analysis, which correlated with the behavioural change in right hand RTs after fatigue. Finally, we used MRSI to quantify potential changes in GABA and Glx. We observed no group mean changes, but on a participant-by-participant basis, GABA decreases in the lM1 and bilateral SMAs correlated with behavioural improvements.

Fatigue increases cross-education

We demonstrated, in line with our hypothesis, that fatiguing contractions performed with the right-hand led to significant behavioural improvements in the left, unfatigued hand. We

observed a significant improvement in left hand RTs, something that was not seen either in the fatigued hand, nor with either hand in the non-fatiguing 5% MVC condition. As would be expected, participants learned the SRTT sequence, as evidenced by a decrease in RTs in sequence blocks in the trained, left-hand. Although against our hypothesis, there was no difference in learning rates between the two conditions, we did observe a fatigue-induced increase in transfer of the learned sequence to the right-hand after left-hand SRTT motor learning, that was not present in the random button presses. There were no additional benefits to the transfer of motor performance (i.e., random block RTs) after fatiguing contractions, yet, both conditions did experience significant CE effects with the untrained right-hand improving RTs in sequence and random blocks.

One plausible explanation for this behavioural effect of transfer of sequence learning is that the increased interhemispheric SMA-SMA connectivity observed after fatigue may facilitate transfer of the motor sequence learned with the left-hand to the right. This-fatigue induced increase in SMA-SMA connectivity may putatively impact neural circuits specifically underpinning sequence learning (Perez *et al.*, 2007), rather than simply motor performance, as no corresponding fatigue-induced improvement in right RTs is observed for the random blocks. Indeed, SMA is known to be involved in consolidation of a learned sequence (Dahms *et al.*, 2020), plays a major role in the planning and self-initiation of voluntary movement, and serves to integrate multimodal information to ensure motor and visual systems are in agreement (Hikosaka *et al.*, 1999; Nakahara *et al.*, 2001). The increased connectivity between left and right SMA in the present study may reflect a mechanism by which fatigue-induced neural changes improve sequence memory for the untrained hand.

At retention there was no difference between the 5% MVC and 50% MVC conditions. This perhaps suggests that fatigue speeds learning in the untrained hand rather than increasing the end magnitude of learning. However, despite not necessarily increasing the total amount of skill acquisition, the finding that fatigue speeds acquisition has implications for motor rehabilitation, where CE is seemingly enhanced in clinical situations (Dragert & Zehr, 2013;

Urbin *et al.*, 2015; Sun *et al.*, 2018), and could therefore be putatively used to speed gains from rehabilitation, something that is of major importance in recovery (Stinear & Byblow, 2014).

Increased functional connectivity between ipsilateral rM1 and rOFC after fatigue

We observed increased functional connectivity between our rM1 seed and the rOFC after fatigue. Increased OFC activity has been associated with faster response times (Bode *et al.*, 2018) and hand motor learning (Alves Heinze *et al.*, 2019). The increased rM1-rOFC functional connectivity observed here may therefore reflect the OFC's role as a top-down motor control region (Ono *et al.*, 2014) which is involved in the regulation of motor responses and error monitoring (Alves Heinze *et al.*, 2019). In line with this hypothesis, Jackson et al. (2003) showed increased activation in the right OFC in participants who significantly improved their performance in a right-hand motor task, either having physically executed the task or having performed motor imagery. Taken together, our results therefore may suggest that increased functional connectivity between the rM1 and the rOFC is functionally relevant for improved RTs in the contralateral, unfatigued left-hand.

Fatigue increased SMA-SMA connectivity

Our ROI-based functional connectivity analysis examined how the temporal correlations between left and right M1 and SMA homologs changed after the right handgrip force-matching task. After fatigue, SMA-SMA functional connectivity increased, and the degree of change was negatively correlated with the degree of fatigue, such that participants who exhibited greater fatigue showed greater increase in SMA-SMA functional connectivity.

The physiological basis of the role of the SMA in CE is not yet clear, but SMA has been described as a 'phylogenetically older' M1 (Goldberg, 1985) which has direct excitatory connections not only onto the M1 circuitry (Shirota *et al.*, 2012; Arai *et al.*, 2012), but onto alpha-motoneurons that innervate the hand and fingers (Maier *et al.*, 2002; Dum & Strick, 2005). The SMA is also an

important region for consolidation and retention of motor sequence learning (Dahms *et al.*, 2020). Therefore, it is plausible that the fatigue-induced increase in SMA-SMA functional connectivity improved CE sequence learning either by influencing rM1 through rSMA-rM1 excitatory connections or through direct corticospinal connections to upper limb alpha-motoneurons (Dum & Strick, 2005). Transcallosal homologous connectivity between motor regions primarily reflects inhibitory processes (Wahl *et al.*, 2007). Therefore, an increase in SMA-SMA functional connectivity may reflect an increase in interhemispheric inhibition between these premotor regions. Previous research has identified the SMA as a critical region for CE (Perez *et al.*, 2007; Ruddy *et al.*, 2017): inhibiting SMA with repetitive TMS abolished CE without impacting SRTT learning with the trained hand. Further, SMA-SMA interhemispheric structural connectivity negatively correlates with the magnitude of CE (Ruddy *et al.*, 2017), such that individuals with greater structural SMA-SMA connectivity exhibit a lower degree of skill transfer. Given this, it is possible that an increase in interhemispheric SMA-SMA functional connectivity, reflecting interhemispheric inhibition, may aid in silencing unwanted cortical activity that facilitates a more focal excitatory process in the opposite hemisphere (Carson, 2020) giving rise to an enhanced CE effect. These interhemispheric network-level effects from the SMA may also be important in the faster response times observed with the left, unfatigued hand following 50% MVC right-hand contractions.

A decrease in lM1 and bilateral SMA GABA after fatigue correlates with improvements in left-hand RTs

To address our hypothesis that fatigue would lead to decreased inhibition in motor regions, we used a novel MRSI sequence to quantify neurochemical concentrations across the sensorimotor network. At a group level, there were no significant GABA changes in M1 and SMA in either hemisphere after fatigue compared with 5% MVC control condition. However, in line with our *a priori* hypothesis, we did observe a significant correlation on a participant-by-participant basis between the decrease in lM1, lSMA, and rSMA GABA after fatigue with the improved behaviour in the unfatigued hand. While the mechanism by which lM1 and bilateral SMA GABA decreases

lead to behavioural improvement in the ipsilateral hand is unclear, a combination of decussated and non-decussated pathways may play an important role (Maruyama *et al.*, 2006; Aboodarda *et al.*, 2016).

Conclusions

This study identified that fatiguing right handgrip contractions led to behavioural improvements in both hands which were accompanied by increased SMA-SMA functional connectivity. In addition, we demonstrated an increase in functional connectivity between rM1 and the rOFC. Speaking to the neurochemical mechanisms underpinning these behavioural improvements in the unfatigued hand, we also demonstrated positive relationships between change in inhibition (GABA) in lM1 and bilateral SMA and a negative relationship between the change in rM1 Glx with the behavioural improvements in the unfatigued left-hand. Taken together, these results suggest that unimanual fatiguing exercise may be a potentially promising adjunct therapy for rehabilitation in a range of neurological or orthopedic conditions.

Author contributions

J.W.A., J.M.L, J.P.F., & C.J.S. conceived and designed the experiment. C.Z. & J.M.L developed the software to run the behavioural experiment. J.W.A., & J.M.L. collected the data and J.W.A., E.C.M., J.M.L., J.P.F., & C.J.S. analyzed the data. All authors were involved in data interpretation. J.W.A. drafted the paper, and all authors revised it and approve the final version.

Conflict of interest

None to report

Funding sources

C.J.S. holds a Sir Henry Dale Fellowship, funded by the Wellcome Trust and the Royal Society (102584/Z/13/Z). This work was also supported by the National Institute for Health Research (NIHR) Oxford Health Biomedical Research Centre, and the John Fell Fund. The Wellcome Centre for Integrative Neuroimaging is supported by core funding from the Wellcome Trust

(203139/Z/16/Z). J.P.F. holds a Natural Sciences and Engineering Research Council of Canada (NSERC) Discovery Grant: RGPIN 2016-0529 at the University of Saskatchewan. J.M.L was supported by a National Institutes of Health Oxford-Cambridge Scholar Fellowship, and the International Biomedical Research Alliance. J.W.A. received an NSERC Alexander Graham Bell Canada Graduate Scholarship – Doctoral (CGS D) Award and a MITACS Globalink Research Award to complete this work.

Acknowledgements

The authors would like to acknowledge Dr. Jason DeFreitas for his valuable insight on the manuscript.

References

Aboodarda SJ, Šambaher N & Behm DG (2016). Unilateral elbow flexion fatigue modulates corticospinal responsiveness in non-fatigued contralateral biceps brachii. *Scand J Med Sci Sport* **26,** 1301–1312.

Allman C, Amadi U, Winkler AM, Wilkins L, Filippini N, Kischka U, Stagg CJ & Johansen-Berg H (2016). Ipsilesional anodal tDCS enhances the functional benefits of rehabilitation in patients after stroke. *Sci Transl Med* **8,** 330re1-330re1.

Alves Heinze R, Vanzella P, Zimeo Morais GA & Sato JR (2019). Hand motor learning in a musical context and prefrontal cortex hemodynamic response: a functional near-infrared spectroscopy (fNIRS) study. *Cogn Process*; DOI: 10.1007/s10339-019-00925-y.

Andersson JLR, Jenkinson M & Smith S (2007*a*). *Non-linear registration aka spatial normalisation FMRIB Technial Report TR07JA2*.

Andersson JLR, Jenkinson M & Smith S (2007*b*). *Non-linear optimisation FMRIB Technial Report TR07JA1*.

Andrushko JW, Gould LA, Renshaw DW, Ekstrand C, Hortobágyi T, Borowsky R & Farthing JP (2021). High force unimanual handgrip contractions increase ipsilateral sensorimotor activation and functional connectivity. *Neuroscience* **452,** 111–125.

Andrushko JW, Lanovaz JL, Björkman KM, Kontulainen SA & Farthing JP (2018). Unilateral strength training leads to muscle-specific sparing effects during opposite homologous limb

531 immobilization. *J Appl Physiol* **124,** 866–876.
532 Arai N, Lu MK, Ugawa Y & Ziemann U (2012). Effective connectivity between human
533 supplementary motor area and primary motor cortex: A paired-coil TMS study. *Exp Brain*
534 *Res* **220,** 79–87.
535 Bachtiar V, Johnstone A, Berrington A, Lemke C, Johansen-Berg H, Emir U & Stagg CJ (2018).
536 Modulating regional motor cortical excitability with noninvasive brain stimulation results
537 in neurochemical changes in bilateral motor cortices. *J Neurosci* **38,** 7327–7336.
538 Bachtiar V, Near J, Johansen-Berg H & Stagg CJ (2015). Modulation of GABA and resting state
539 functional connectivity by transcranial direct current stimulation. *Elife* **4,** e08789.
540 Bode S, Bennett D, Sewell DK, Paton B, Egan GF, Smith PL & Murawski C (2018). Dissociating
541 neural variability related to stimulus quality and response times in perceptual decision-
542 making. *Neuropsychologia* **111,** 190–200.
543 Cabanes E, Confort-Gouny S, Le Fur Y, Simond G & Cozzone PJ (2001). Optimization of residual
544 water signal removal by HLSVD on simulated short echo time proton MR spectra of the
545 human brain. *J Magn Reson* **150,** 116–125.
546 Carr JC, Bemben M, Stock MS & DeFreitas JM (2021). Ipsilateral and contralateral responses
547 following unimanual fatigue with and without illusionary mirror visual feedback. *J*
548 *Neurophysiol*jn.00077.2021.
549 Carson RG (2020). Inter-hemispheric inhibition sculpts the output of neural circuits by co-opting
550 the two cerebral hemispheres. *J Physiol*JP279793.
551 Cox RW (1996). AFNI: software for analysis and visualization of functional magnetic resonance
552 neuroimages. *Comput Biomed Res* **29,** 162–173.
553 Cox RW & Glen DR (2013). Nonlinear warping in AFNI. *Present 19th Annu Meet Organ Hum*
554 *Brain Mapp*. Available at:
555 https://afni.nimh.nih.gov/pub/dist/HBM2013/Cox_Poster_HBM2013.pdf.
556 Dahms C, Brodoehl S, Witte OW & Klingner CM (2020). The importance of different learning
557 stages for motor sequence learning after stroke. *Hum Brain Mapp* **41,** 270–286.
558 Dehno SN, Kamali F, Shariat A & Jaberzadeh S (2021). Unilateral strength training of the less
559 affected hand improves cortical excitability and clinical outcomes in patients with subacute

560 stroke: A randomized controlled trial. *Arch Phys Med Rehabil*; DOI:
561 10.1016/j.apmr.2020.12.012.
562 Dragert K & Zehr EP (2013). High-intensity unilateral dorsiflexor resistance training results in
563 bilateral neuromuscular plasticity after stroke. *Exp Brain Res* **225,** 93–104.
564 Dum RP & Strick PL (2005). Frontal lobe inputs to the digit representations of the motor areas
565 on the lateral surface of the hemisphere. *J Neurosci* **25,** 1375–1386.
566 Emir UE, Burns B, Chiew M, Jezzard P & Thomas MA (2017). Non-water-suppressed
567 short-echo-time magnetic resonance spectroscopic imaging using a concentric ring k-space
568 trajectory. *Nmr Biomed*; DOI: 10.1002/NBM.3714.
569 Farthing JP, Krentz JR & Magnus CR (2009). Strength training the free limb attenuates strength
570 loss during unilateral immobilization. *J Appl Physiol* **106,** 830–836.
571 Farthing JP, Krentz JR, Magnus CR, Barss TS, Lanovaz JL, Cummine J, Esopenko C, Sarty GE &
572 Borowsky R (2011). Changes in functional magnetic resonance imaging cortical activation
573 with cross education to an immobilized limb. *Med Sci Sports Exerc* **43,** 1394–1405.
574 Floyer-Lea A, Wylezinska M, Kincses T & Matthews PM (2006). Rapid modulation of GABA
575 concentration in human sensorimotor cortex during motor learning. *J Neurophysiol* **95,**
576 1639–1644.
577 Goldberg G (1985). Supplementary motor area structure and function: Review and hypotheses.
578 *Behav Brain Sci* **8,** 567–588.
579 Griffanti L, Salimi-Khorshidi G, Beckmann CF, Auerbach EJ, Douaud G, Sexton CE, Zsoldos E,
580 Ebmeier KP, Filippini N, Mackay CE, Moeller S, Xu J, Yacoub E, Baselli G, Ugurbil K, Miller KL
581 & Smith SM (2014). ICA-based artefact removal and accelerated fMRI acquisition for
582 improved resting state network imaging. *Neuroimage*; DOI:
583 10.1016/j.neuroimage.2014.03.034.
584 Hikosaka O, Sakai K, Lu X, Nakahara H, Rand MK, Nakamura K, Miyachi S & Doya K (1999).
585 Parallel neural networks for learning sequential procedures. *Trends Neurosci* **22,** 464–471.
586 Available at: http://www.cell.com/article/S0166223699014393/fulltext [Accessed April 15,
587 2021].
588 Jackson PL, Lafleur MF, Malouin F, Richards CL & Doyon J (2003). Functional cerebral

589 reorganization following motor sequence learning through mental practice with motor
590 imagery. *Neuroimage*; DOI: 10.1016/S1053-8119(03)00369-0.
591 Jenkinson M, Bannister P, Brady M & Smith S (2002). Improved optimization for the robust and
592 accurate linear registration and motion correction of brain images. *Neuroimage* **17,** 825–
593 841.
594 Jenkinson M, Beckmann CF, Behrens TEJ, Woolrich MW & Smith SM (2012). FSL. *Neuroimage*
595 **62,** 782–790.
596 Jenkinson M & Smith S (2001). A global optimisation method for robust affine registration of
597 brain images. *Med Image Anal* **5,** 143–156.
598 Jiang Z, Wang X-F, Kisiel-Sajewicz K, Yan JH & Yue GH (2012). Strengthened functional
599 connectivity in the brain during muscle fatigue. *Neuroimage* **60,** 728–737.
600 Johansen-Berg H, Behrens TEJ, Robson MD, Drobnjak I, Rushworth MFS, Brady JM, Smith SM,
601 Higham DJ & Matthews PM (2004). Changes in connectivity profiles define functionally
602 distinct regions in human medial frontal cortex. *Proc Natl Acad Sci U S A* **101,** 13335–
603 13340.
604 Kim D-Y, Lim J-Y, Kang EK, You DS, Oh M-K, Oh B-M & Paik N-J (2010). Effect of transcranial
605 direct current stimulation on motor recovery in patients with subacute stroke. *Am J Phys*
606 *Med Rehabil* **89,** 879–886.
607 Kleiner M, Brainard DH, Pelli DG, Broussard C, Wolf T & Niehorster D (2007). What's new in
608 Psychtoolbox-3? *Perception*.
609 Klose U (1990). In vivo proton spectroscopy in presence of eddy currents. *Magn Reson Med* **14,**
610 26–30.
611 Kolasinski J, Hinson EL, Divanbeighi Zand AP, Rizov A, Emir UE & Stagg CJ (2019). The dynamics
612 of cortical GABA in human motor learning. *J Physiol*; DOI: 10.1113/JP276626.
613 Magnus CR, Arnold CM, Johnston G, Dal-Bello Haas V, Basran J, Krentz JR & Farthing JP (2013).
614 Cross-education for improving strength and mobility after distal radius fractures: A
615 randomized controlled trial. *Arch Phys Med Rehabil* **94,** 1247–1255.
616 Magnus CR, Barss TS, Lanovaz JL & Farthing JP (2010). Effects of cross-education on the muscle
617 after a period of unilateral limb immobilization using a shoulder sling and swathe. *J Appl*

618 *Physiol* **109,** 1887–1894.
619 Maier MA, Armand J, Kirkwood PA, Yang H-W, Davis JN & Lemon R.N. (2002). Differences in the
620 corticospinal projection from primary motor cortex and supplementary motor area to
621 macaque upper limb motoneurons: An anatomical and electrophysiological study. *Cereb*
622 *Cortex* **12,** 281–296.
623 Manca A, Hortobágyi T, Carroll TJ, Enoka RM, Farthing JP, Gandevia SC, Kidgell DJ, Taylor JL &
624 Deriu F (2021). Contralateral effects of unilateral strength and skill training: Modified
625 delphi consensus to establish key aspects of cross-education. *Sport Med* **51,** 11–20.
626 Manca A, Hortobágyi T, Rothwell J & Deriu F (2018). Neurophysiological adaptations in the
627 untrained side in conjunction with cross-education of muscle strength: a systematic review
628 and meta-analysis. *J Appl Physiol* **124,** 1502–1518.
629 Maruyama A, Matsunaga K, Tanaka N & Rothwell JC (2006). Muscle fatigue decreases short-
630 interval intracortical inhibition after exhaustive intermittent tasks. *Clin Neurophysiol* **117,**
631 864–870.
632 Maruyama A, Nuruki A, Etoh S & Rothwell JC (2012). Could fatigue be used as a paradoxical
633 intervention to improve motor learning after stroke? In *International Conference on*
634 *Complex Medical Engineering*, pp. 298–301. IEEE. Available at:
635 http://ieeexplore.ieee.org/document/6275681/.
636 Miller KL et al. (2016). Multimodal population brain imaging in the UK Biobank prospective
637 epidemiological study. *Nat Neurosci 2016 1911* **19,** 1523–1536.
638 Nakahara H, Doya K & Hikosaka O (2001). Parallel cortico-basal ganglia mechanisms for
639 acquisition and execution of visuomotor sequences - A computational approach. *J Cogn*
640 *Neurosci* **13,** 626–647.
641 Ni Z, Gunraj C & Chen R (2007). Short interval intracortical inhibition and facilitation during the
642 silent period in human. *J Physiol* **583,** 971–982.
643 Ono Y, Nomoto Y, Tanaka S, Sato K, Shimada S, Tachibana A, Bronner S & Noah JA (2014).
644 Frontotemporal oxyhemoglobin dynamics predict performance accuracy of dance
645 simulation gameplay: Temporal characteristics of top-down and bottom-up cortical
646 activities. *Neuroimage* **85,** 461–470.

Pearce AJ, Hendy AM, Bowen WA & Kidgell DJ (2013). Corticospinal adaptations and strength maintenance in the immobilized arm following 3 weeks unilateral strength training. *Scand J Med Sci Sport* **23,** 740–748.

Peirce J, Gray JR, Simpson S, MacAskill M, Höchenberger R, Sogo H, Kastman E & Lindeløv JK (2019). PsychoPy2: Experiments in behavior made easy. *Behav Res Methods* **51,** 195–203.

Pelet DCS & Orsatti FL (2021). Effects of resistance training at different intensities of load on cross-education of muscle strength. *Appl Physiol Nutr Metab*apnm-2021-0088.

Perez MA, Tanaka S, Wise SP, Sadato N, Tanabe HC, Willingham DT & Cohen LG (2007). Neural substrates of intermanual transfer of a newly acquired motor skill. *Curr Biol* **17,** 1896–1902.

Provencher SW (2001). Automatic quantitation of localized in vivo 1H spectra with LCModel. *NMR Biomed* **14,** 260–264.

Provencher SW (2016). LCModel and LCMgui User's Manual. Available at: http://s-provencher.com/lcm-manual.shtml.

Reis J, Schambra HM, Cohen LG, Buch ER, Fritsch B, Zarahn E, Celnik PA & Krakauer JW (2009). Noninvasive cortical stimulation enhances motor skill acquisition over multiple days through an effect on consolidation. *Proc Natl Acad Sci U S A* **106,** 1590–1595.

Ruddy KL & Carson RG (2013). Neural pathways mediating cross education of motor function. *Front Hum Neurosci* **7,** 1–22.

Ruddy KL, Leemans A, Woolley DG, Wenderoth N & Carson RG (2017). Structural and functional cortical connectivity mediating cross education of motor function. *J Neurosci* **37,** 2555–2564.

Saad ZS, Glen DR, Chen G, Beauchamp MS, Desai R & Cox RW (2009). A New Method for Improving Functional-to-Structural MRI Alignment using Local Pearson Correlation. *Neuroimage* **44,** 839.

Salimi-Khorshidi G, Douaud G, Beckmann CF, Glasser MF, Griffanti L & Smith SM (2014). Automatic denoising of functional MRI data: Combining independent component analysis and hierarchical fusion of classifiers. *Neuroimage* **90,** 449–468.

Shirota Y, Hamada M, Terao Y, Ohminami S, Tsutsumi R, Ugawa Y & Hanajima R (2012).

676 Increased primary motor cortical excitability by a single-pulse transcranial magnetic
677 stimulation over the supplementary motor area. *Exp Brain Res* **219,** 339–349.
678 Smith SM (2002). Fast robust automated brain extraction. *Hum Brain Mapp* **17,** 143–155.
679 Stagg CJ, Bachtiar V, Amadi U, Gudberg CA, Ilie AS, Sampaio-Baptista C, O'Shea J, Woolrich M,
680 Smith SM, Filippini N, Near J & Johansen-Berg H (2014). Local GABA concentration is
681 related to network-level resting functional connectivity. *Elife* **3,** 1–9.
682 Stagg CJ, Bachtiar V & Johansen-Berg H (2011*a*). The role of GABA in human motor learning.
683 *Curr Biol* **21,** 480–484.
684 Stagg CJ, Jayaram G, Pastor D, Kincses ZT, Matthews PM & Johansen-Berg H (2011*b*). Polarity
685 and timing-dependent effects of transcranial direct current stimulation in explicit motor
686 learning. *Neuropsychologia* **49,** 800–804.
687 Steel A, Chiew M, Jezzard P, Voets NL, Plaha P, Thomas MA, Stagg CJ & Emir UE (2018).
688 Metabolite-cycled density-weighted concentric rings k-space trajectory (DW-CRT) enables
689 high-resolution 1 H magnetic resonance spectroscopic imaging at 3-Tesla. *Sci Rep* **8,** 7792.
690 Stinear CM & Byblow WD (2014). Predicting and accelerating motor recovery after stroke. *Curr*
691 *Opin Neurol* **27,** 624–630.
692 Sun Y, Ledwell NMH, Boyd LA & Zehr EP (2018). Unilateral wrist extension training after stroke
693 improves strength and neural plasticity in both arms. *Exp Brain Res* **236,** 2009–2021.
694 Takahashi K, Maruyama A, Maeda M, Etoh S, Hirakoba K, Kawahira K & Rothwell JC (2009).
695 Unilateral grip fatigue reduces short interval intracortical inhibition in ipsilateral primary
696 motor cortex. *Clin Neurophysiol* **120,** 198–203.
697 The Jamovi Project (2020). Jamovi (Version 1.2). Available at: https://www.jamovi.org.
698 The Mathworks Inc (2018). MATLAB 2018a. *WwwMathworksCom/Products/Matlab*.
699 Urbin MA, Harris-Love ML, Carter AR & Lang CE (2015). High-intensity, unilateral resistance
700 training of a non-paretic muscle group increases active range of motion in a severely
701 paretic upper extremity muscle group after stroke. *Front Neurol* **6,** 119.
702 Valdes O, Ramirez C, Perez F, Garcia-Vicencio S, Nosaka K & Penailillo L (2021). Contralateral
703 effects of eccentric resistance training on immobilized arm. *Scand J Med Sci Sports* **31,** 76–
704 90.

705 Wahl M, Lauterbach-Soon B, Hattingen E, Jung P, Singer O, Volz S, Klein JC, Steinmetz H &
706 Ziemann U (2007). Human motor corpus callosum: Topography, somatotopy, and link
707 between microstructure and function. *J Neurosci* **27,** 12132–12138.
708 Walsh DO, Gmitro AF & Marcellin MW (2000). Adaptive reconstruction of phased array MR
709 imagery. *Magn Reson Med*; DOI: 10.1002/(SICI)1522-2594(200005)43:5.
710 Weinrich CA, Brittain JS, Nowak M, Salimi-Khorshidi R, Brown P & Stagg CJ (2017). Modulation
711 of long-range connectivity patterns via frequency-specific stimulation of human cortex.
712 *Curr Biol* **27,** 3061-3068.e3.
713 Woolrich MW, Behrens TEJ, Beckmann CF, Jenkinson M & Smith SM (2004). Multilevel linear
714 modelling for FMRI group analysis using Bayesian inference. *Neuroimage* **21,** 1732–1747.
715 Woolrich MW, Ripley BD, Brady M & Smith SM (2001). Temporal autocorrelation in univariate
716 linear modeling of FMRI data. *Neuroimage* **14,** 1370–1386.
717

718 **Figure legends**

719 **Figure 1. A)** Theoretical physiological model for the present study, **B)** Schematic outlining the
720 study design. Both aspects of this figure were created with BioRender.com.

721

722 **Figure 2.** Behavioural changes. **A)** Beta values for the area under the curve of the force profile
723 from the nine-minute right handgrip force-matching task in experiment one. * = 50% MVC
724 experienced a significant decline in motor performance (one-sample *t*-test, $p = 0.005$), ** =
725 significant difference between conditions (paired-samples *t*-test, $p = 0.006$), and **B)** Percent
726 change in response times from Pre-MRI to Post-MRI for the left (purple data points) and right
727 (green data points) hands after the right-hand force-matching task at 5% MVC (circles) and 50%
728 MVC (triangles). † = significant condition × hand interaction ($p = 0.045$),** = significant paired
729 sample *t*-test ($p = 0.037$),* = significant one-sample *t*-test change in response times ($p = 0.009$).
730 Schematic of study design was created with BioRender.com.

731

732 **Figure 3. A)** SRTT motor learning blocks across time with the trained left-hand. R = random
733 trials, S = sequence trials, error bars = 95% confidence intervals, and **B)** Difference in response
734 times between random blocks and the sequence block for the left (left side; purple data points)
735 and right hands (right side; green data points) at Post-Learning (top row) and Retention
736 (bottom row) for the 5% MVC (circles) and 50% MVC (triangles) conditions. * = significant
737 difference between sequence and random blocks (all $p < 0.05$), † = significant interaction
738 between conditions at Post Learning for the right hand ($p = 0.025$). Schematic of study design
739 was created with BioRender.com.

740

741 **Figure 4.** Functional connectivity analyses for **A)** Seed-based functional connectivity analysis
742 between the right ipsilateral primary motor cortex (seed) and the rest of the brain in the 50%
743 MVC condition, data is a Z-statistic threshold map in standard space. Z-threshold = 3.1. Figure is
744 in radiological view (left on right, right on left). **B)** Change in interhemispheric functional
745 connectivity between contralateral and ipsilateral primary motor cortices (M1-M1; red data
746 points), and the contralateral and ipsilateral supplementary motor areas (SMA-SMA; orange

data points) for 5% MVC (circles) and 50% MVC (triangles). Back horizonal bar represents the mean change. Grey shaded area represents the standard deviation. † = significant condition × ROI × time interaction (p = 0.007), ** = significant ROI × time interaction for 50% MVC condition (p = 0.004) * = significant paired-sample t-test against (SMA-SMA; p = 0.045), and **C)** Scatter plot correlation between X-axis: The change in interhemispheric functional connectivity z-scores between the contralateral left and ipsilateral right supplementary motor areas (SMA-SMA) and Y-axis: beta values representing the decline in motor performance over time (negative slope = performance decline over time) ($r^2_{adjusted}$ = 0.208, p = 0.050, β = -0.1572). Schematic of study design was created with BioRender.com.

Figure 5. A) Magnetic resonance spectroscopic imaging spectrum from a representative participant, with spectra from M1 voxels in each hemisphere. **B)** Scatter plot correlations for the right hemisphere (purple) and left hemisphere (green) between X-axes: SMA (top scatter plots), M1 (bottom scatter plots) for GABA/tCr (rSMA, lSMA, lM1) and Glx/tCr (rM1) ratios with Y-axes: the change in left-hand response times (ms) after performing the right-hand target matching task at either 5% MVC (circles) or 50% MVC (triangles) conditions. Schematic of study design was created with BioRender.com.

Table 1. Post > Pre-force-matching task rs-fMRI contrasts from iM1 seed-based functional connectivity analysis

50% MVC						
			MNI Coordinates (mm)			
Voxels	***p*-value**	**z-max**	**X**	**Y**	**Z**	**Label**
104	0.0348	5.12	34	26	-6	Right Orbitofrontal Cortex
5% MVC						
			MNI Coordinates (mm)			
Voxels	***p*-value**	**z-max**	**X**	**Y**	**Z**	**Label**
182	0.00187	4.44	28	-50	-26	Right Cerebellum VI
104	0.0363	4.78	-42	-54	-4	Left Inferior Temporal Gyrus

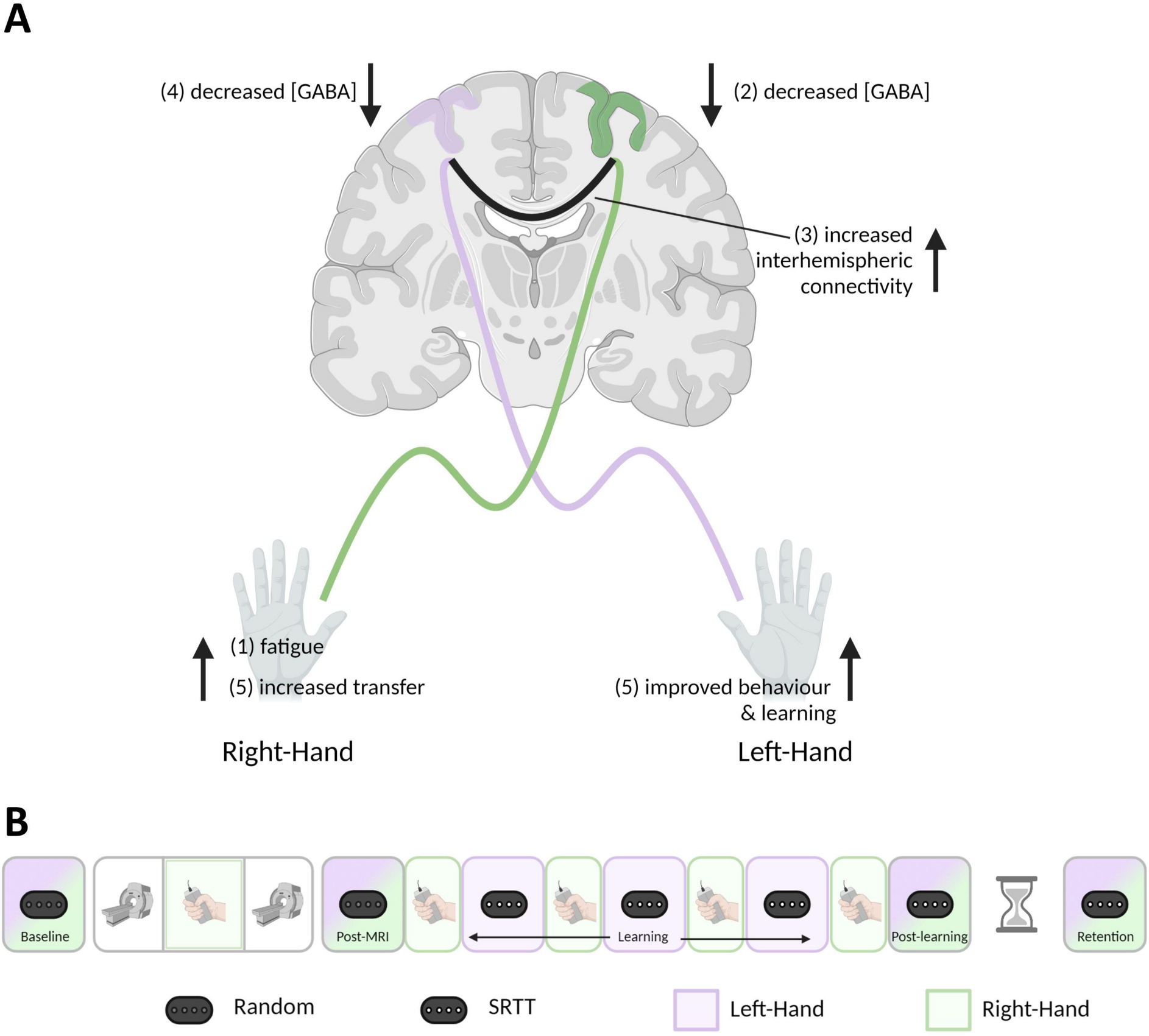
A
(4) decreased [GABA]
(2) decreased [GABA]
(3) increased interhemispheric connectivity
(1) fatigue
(5) increased transfer
(5) improved behaviour & learning
Right-Hand
Left-Hand
B
Baseline
Post-MRI
Learning
Post-learning
Retention
Random
SRTT
Left-Hand
Right-Hand

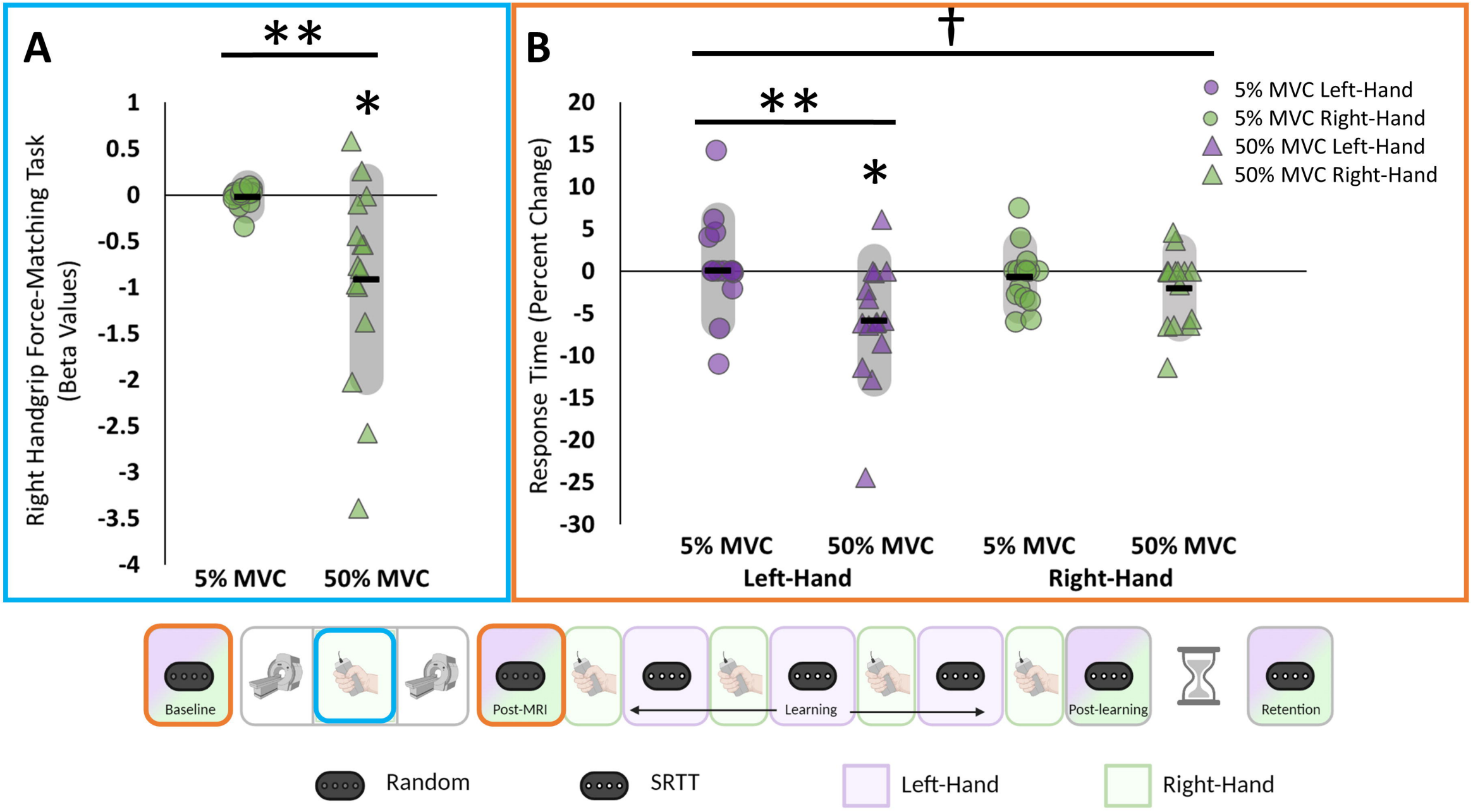
A
**
*
Right Handgrip Force-Matching Task (Beta Values)
1
0.5
0
-0.5
-1
-1.5
-2
-2.5
-3
-3.5
-4
5% MVC
50% MVC
B
†
**
*
Response Time (Percent Change)
20
15
10
5
0
-5
-10
-15
-20
-25
-30
5% MVC Left-Hand
5% MVC Right-Hand
50% MVC Left-Hand
50% MVC Right-Hand
5% MVC
50% MVC
5% MVC
50% MVC
Left-Hand
Right-Hand
Baseline
Post-MRI
Learning
Post-learning
Retention
Random
SRTT
Left-Hand
Right-Hand

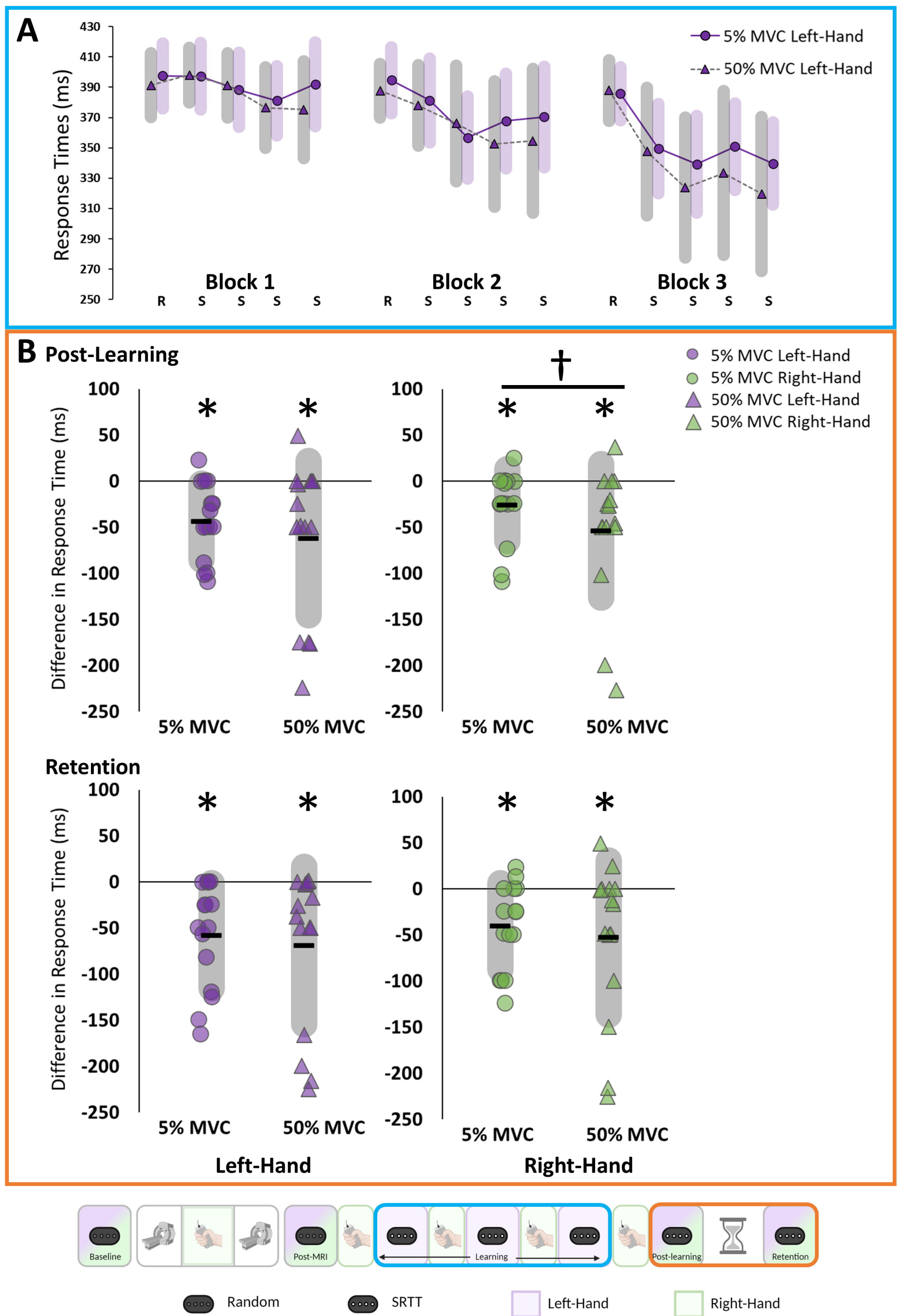
A
Response Times (ms)
430
410
390
370
350
330
310
290
270
250
5% MVC Left-Hand
50% MVC Left-Hand
Block 1
Block 2
Block 3
R S S S S
B Post-Learning
Retention
Difference in Response Time (ms)
100
50
0
-50
-100
-150
-200
-250
5% MVC
50% MVC
Left-Hand
Right-Hand
5% MVC Left-Hand
5% MVC Right-Hand
50% MVC Left-Hand
50% MVC Right-Hand
Baseline
Post-MRI
Learning
Post-learning
Retention
Random
SRTT
Left-Hand
Right-Hand

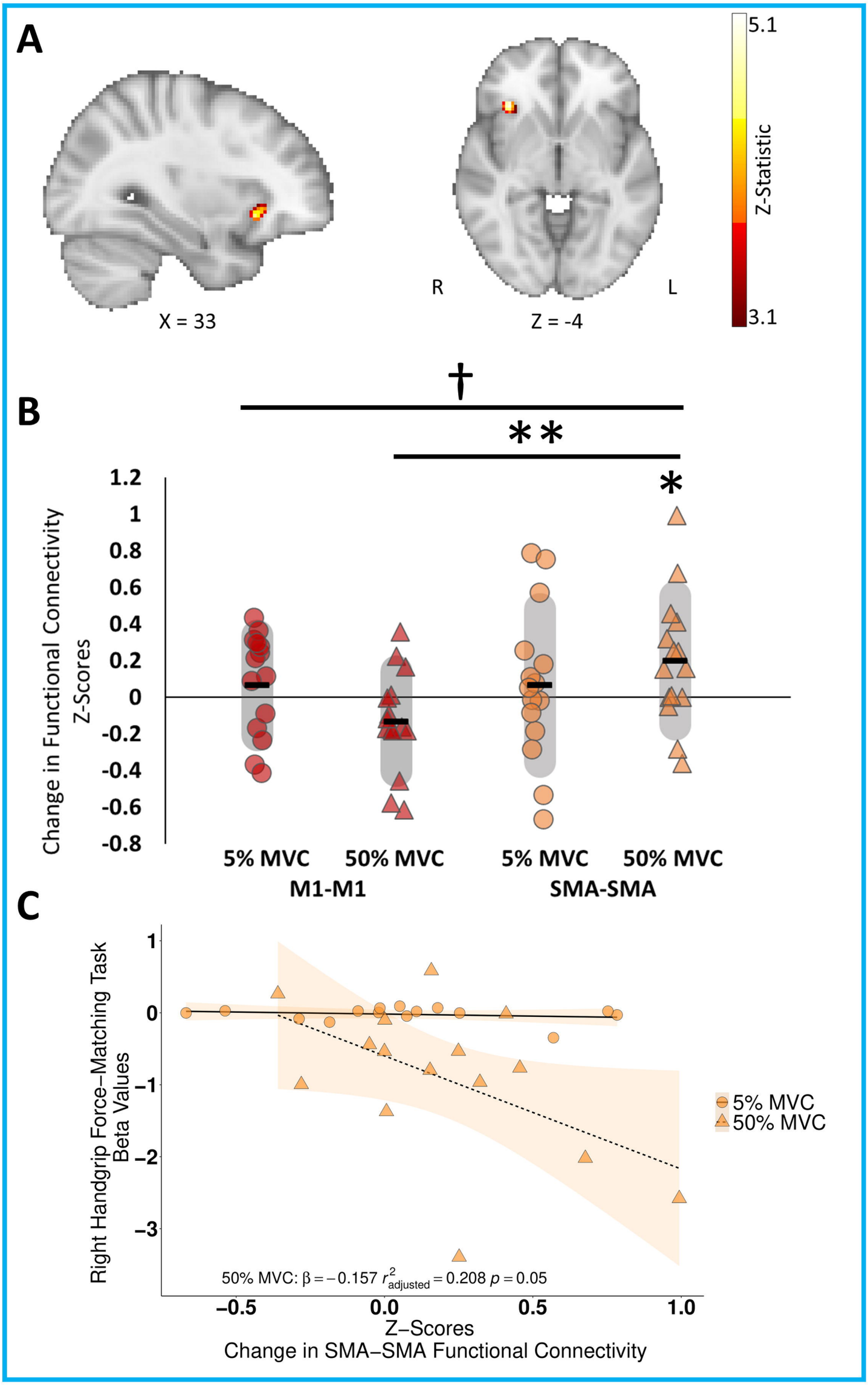
A
X = 33
R
L
Z = -4
5.1
Z-Statistic
3.1
B
†
**
*
Change in Functional Connectivity
Z-Scores
1.2
1
0.8
0.6
0.4
0.2
0
-0.2
-0.4
-0.6
-0.8
5% MVC
50% MVC
5% MVC
50% MVC
M1-M1
SMA-SMA
C
Right Handgrip Force–Matching Task
Beta Values
1
0
−1
−2
−3
50% MVC: β = −0.157 $r^2_{adjusted}$ = 0.208 p = 0.05
−0.5
0.0
0.5
1.0
Z–Scores
Change in SMA–SMA Functional Connectivity
5% MVC
50% MVC

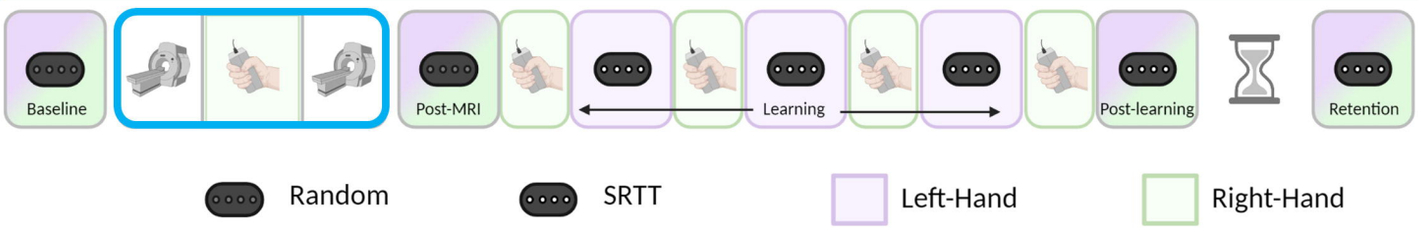
Baseline
Post-MRI
Learning
Post-learning
Retention
Random
SRTT
Left-Hand
Right-Hand

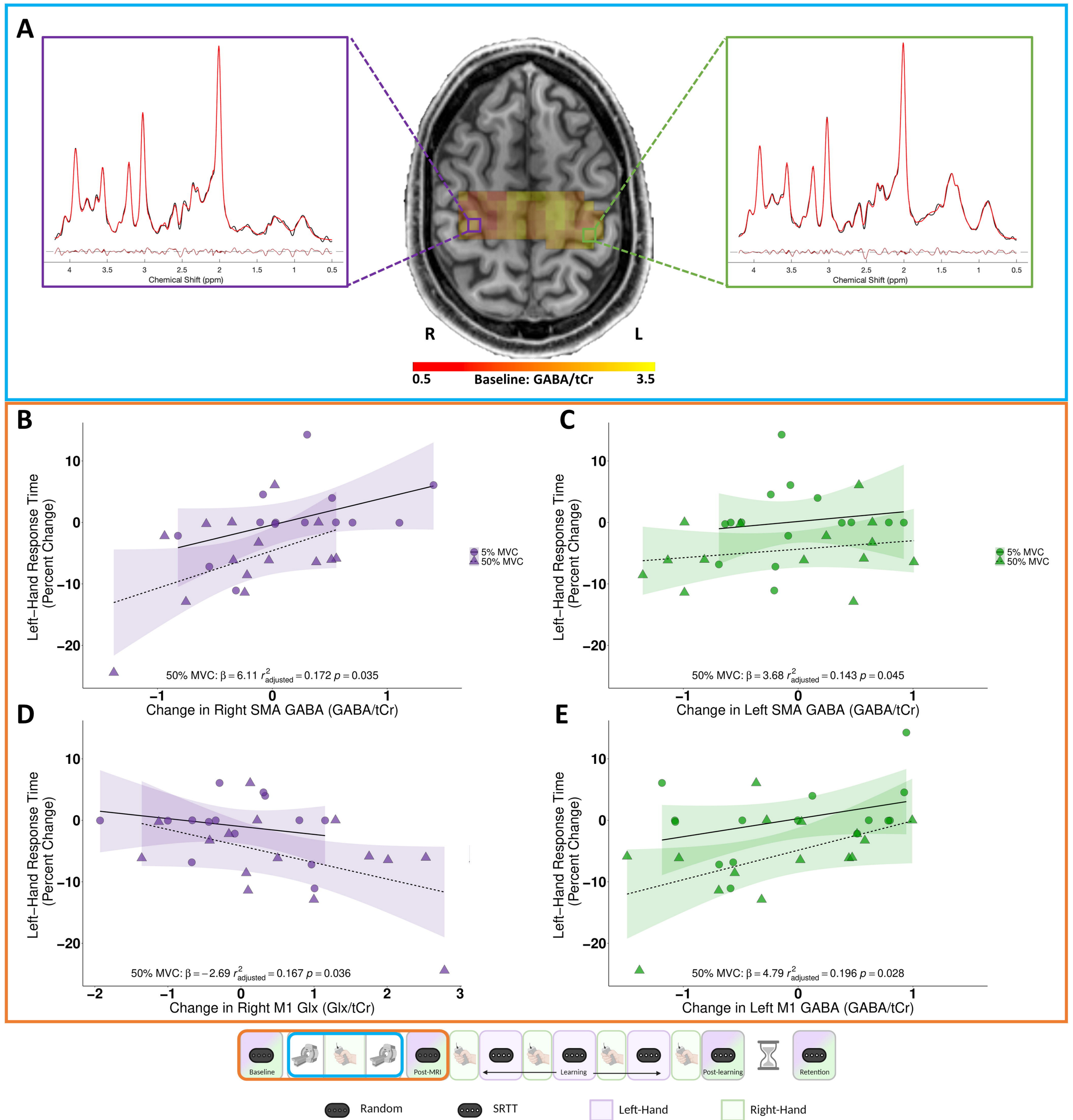
A
Chemical Shift (ppm)
R
L
0.5
Baseline: GABA/tCr
3.5
B
Left–Hand Response Time (Percent Change)
Change in Right SMA GABA (GABA/tCr)
5% MVC
50% MVC
50% MVC: β = 6.11 $r^2_{adjusted}$ = 0.172 p = 0.035
C
Change in Left SMA GABA (GABA/tCr)
50% MVC: β = 3.68 $r^2_{adjusted}$ = 0.143 p = 0.045
D
Change in Right M1 Glx (Glx/tCr)
50% MVC: β = −2.69 $r^2_{adjusted}$ = 0.167 p = 0.036
E
Change in Left M1 GABA (GABA/tCr)
50% MVC: β = 4.79 $r^2_{adjusted}$ = 0.196 p = 0.028
Baseline
Post-MRI
Learning
Post-learning
Retention
Random
SRTT
Left-Hand
Right-Hand